Host-encoded DNA methyltransferases modify the epigenome and host tropism of invading phages

Michiko Takahashi,[a#] Satoshi Hiraoka,[b] Yuki Matsumoto,[c] Rikako Shibagaki,[a] Takako Ujihara,[d] Hiromichi Maeda,[a] Satoru Seo,[a] Keizo Nagasaki,[c] Hiroaki Takeuchi,[e] Shigenobu Matsuzaki[f]

[a]Department of Surgery, Kochi Medical School, Kochi University, Nankoku, Kochi, Japan

[b]Research Center for Bioscience and Nanoscience (CeBN), Research Institute for Marine Resources Utilization, Japan Agency for Marine-Earth Science and Technology (JAMSTEC), Yokosuka, Kanagawa, Japan

[c]Faculty of Agriculture and Marine Science, Kochi University, Nankoku, Kochi, Japan

[d]Science Research Center, Kochi University, Nankoku, Kochi, Japan

[e]Department of Medical Laboratory Sciences, Health and Science, International University of Health and Welfare Graduate School, Narita, Chiba, Japan

[f]Faculty of Health Sciences, Kochi Gakuen University, Kochi, Kochi, Japan

Running Head: DNA methylation of host bacteria and adapted phages

[#]Address correspondence to Michiko Takahashi, michikot@kochi-u.ac.jp.

Michiko Takahashi and Satoshi Hiraoka contributed equally to this work. Author order was determined based on correspondence to this work.

Word counts for the abstract and text: 4942

Abstract

A part of prokaryotic DNA methyltransferases (MTases) is associated with phage-defense systems (e.g., restriction-modification [RM] system) to combat the invasion of foreign DNA (e.g., phages). To date, the epigenomes of host and phage during the infection cycle have not been directly observed, and their association with phage infection efficiency remains unclear. Here, using the wide-host-range phage KHP30T and three *Helicobacter pylori* strains (26695, 3401T, and HPK5) that possess different sets of MTases, we investigated changes in infection efficiency and epigenomes of the phage via adaptation to each host strain. Based on the designed multi-stage infection flow, adapted phages showed higher titers only against the last infected *H. pylori* strain, suggesting an attendant change in host tropism. Using single-molecule real-time sequencing, we retrieved each complete genome and 15 and 20 methylated motifs from *H. pylori* 3401T and HPK5, respectively. In general, the methylated motifs were common between pairs of adapted phages and the last infected host strain. Some exceptions were identified that may arise from phase variation. Our results demonstrate phage genomes are methylated by host-encoded MTases during the infection cycle as they pass through the host RM system, resulting in increased infection efficiency of phages against the same host strain.

Importance

The restriction–modification (RM) system has a great impact on host-phage interactions in nature. Single molecule real-time sequencing is invaluable for identifying DNA methylation in prokaryotic and viral genomes. However, no studies have compared DNA modification between host prokaryotes and infecting phages. Here, to model bacteria–phage interactions mediated by host-encoded MTases, we performed titration of adapted phages via a multi-stage infection flow together with direct observation of the epigenomes of both bacterial host and phage. We believe that such an approach would enhance our understanding of microbial ecology.

Keywords

Epigenome, Restriction-modification system, Phage-host interaction, SMRT sequencing, *Helicobacter pylori*

Introduction

DNA methylation modification catalyzed by methyltransferases (MTases) is a universal cellular process of epigenetic regulation in all three kingdoms of life and viruses (1). In prokaryotes, DNA methylation generally occurs in three forms; N6-methyladenine (m6A), C5-methylcytosine (m5C), and N4-methylcytosine (m4C) (2, 3). A part of prokaryotic MTases is associated with restriction-modification (RM) systems that defend against foreign DNA such as conjugative plasmids and phages (4–6). Most of these systems comprise a MTase and restriction endonuclease (REase) that recognizes a specific target sequence for cleavage. These RM systems are classified as Type I, II, and III according to their subunit composition, cofactor requirements, structure of their recognition sequence, and mode of action (7). The REase interacts with its target DNA sequence to cleave the DNA, whereas the MTase methylates the recognition site to protect the site from cleavage (7). Consequently, host genomic DNA is methylated by the endogenous MTase and protected against REase digestion, while unmethylated foreign DNAs will be subject to cleavage by the REase (7, 8). In contrast to the three major groups, Type IV systems are made up of only REase(s), which recognize and cleave methylated DNAs (7, 8).

Apart from the RM systems, other phage defense systems possibly mediated by DNA methylation have recently been discovered, e.g., BREX (9) and DISARM (10). In addition to these defense systems, DNA methylation also contributes to various physiological functions such as asymmetric cell division (11, 12), motility (13), and pathogen virulence (14–16). Thus, methylation-mediated biological processes have an impact on a wide range of microbial ecology including phage-host interactions. Indeed, there has been growing interest in epigenomic systems among diverse prokaryotes and viruses given their importance in microbial physiology, genetics, evolution, and ecology (17–19).

86 Phages occasionally evade a host's defense system(s), allowing them to
87 successfully multiply in cells of the same host strain (20, 21). Thus, against the same
88 bacterial strain these so-called adapted phages show increased infectious titer. Based on
89 cultivation and infection experiments using well-characterized microbes with authentic
90 RM systems (e.g., *Escherichia coli*, *Bacillus subtilis*, *Haemophilus* spp, and *Salmonella*
91 spp.), it is believed that phage genomes are modified by MTases encoded on the host
92 genome during infection. Hence, the adapted phages grab a 'protective suit' against the
93 host RM system, although the phage is still restricted by other strains with different sets
94 of MTases (22). The development of single molecule real-time (SMRT) sequencing has
95 proved to be invaluable for detecting DNA modifications (23–30). However, to the best
96 of our knowledge, there have been no reports that directly compared the epigenomes of
97 the same phage strain after infection with different host strains.
98 We previously reported KHP30, a double-stranded DNA phage belonging to the
99 *Schmidvirus* genus (31–33) that infects *Helicobacter pylori*. KHP30, which shows a
100 wide-range of host specificity, has a pseudolysogenic life cycle in which the phage
101 genome forms an episome in the host cell rather than integrating into its genome (32).
102 Despite their small genome size, *H. pylori* harbors multiple RM systems with high
103 compositional variation, resulting in highly diverse methylomes (34–36). However, no
104 epigenomic evaluation has been performed whether the MTases encoded in the *H. pylori*
105 genome function against invading phages. Based on these considerations, we reasoned
106 that KHP30 and *H. pylori* is an appropriate model for investigating methylation-mediated
107 phage-host interactions.
108 Here, we investigated the infection efficiency and epigenomic changes of
109 KHP30T phages (derived from KHP30) adapted to three *H. pylori* strains (26695, 3401T,
110 and HPK5) that harbor different sets of MTases via a designed multi-stage infection flows
111 (Fig. 1). Our results highlighted that the adapted phages showed high infectious titers
112 against strains of *H. pylori* that the phage infected in the last generation, but low titers
113 against other strains. Epigenomic analysis revealed methylated motifs on the KHP30T
114 genome were shared with those of the last adapted *H. pylori* strains. These findings

115 suggest that the phage genome was modified by host-encoded MTases, resulting in the
116 phage DNA evading cleavage by the cognate REases. The modified phage showed
117 increased infection efficiency in the same bacterial strain.
118
119 **Results**
120 **Titration of adapted phages**
121 We designed multi-stage infection flows using KHP30T phage and three *H.*
122 *pylori* strains (26695, 3401T, and HPK5) to obtain adapted phages with different infection
123 histories (Fig. 1, Fig. S1). Using this strategy, we retrieved nine adapted phages (K2, K23,
124 K232, K23H, K23H3, K2H, K2H2, K2H3, K2H3H). For example, K23 represents a
125 KHP30T phage adapted to *H. pylori* 26695 in the first stage and to *H. pylori* 3401T in the
126 second stage. Infectious titers were then determined using plaque assay. Adapted phages
127 showed high titers against *H. pylori* strains that the phage infected in the last generation,
128 but low titers against non- or previously-adapted hosts (Fig. 2, S2). For example, K2, the
129 phage adapted to *H. pylori* 26695 in the first stage (Fig. 1), showed a significantly higher
130 titer (9.2 $\log_{10}$ plaque forming units [PFU]/mL) against 26695, but a markedly lower titer
131 against 3401T and HPK5 (3.1 and 3.9 log PFU/mL, respectively) ($p < 0.01$, Tukey–
132 Kramer test). Focusing on second-stage phages, K23 showed a significantly higher titer
133 (8.9 $\log_{10}$ PFU/mL) against *H. pylori* 3401T than against 26695 and HPK5 (0.8, and 1.8
134 $\log_{10}$ PFU/mL, respectively) ($p < 0.01$), even though K23 had adapted to 26695 in the
135 first stage. K2H also showed the same trend: a titer against *H. pylori* HPK5 (8.2 $\log_{10}$
136 PFU/mL) that was significantly higher than against 26695 and 3401T (1.9 and 2.4 $\log_{10}$
137 PFU/mL, respectively) ($p < 0.01$).
138 Similarly, third-stage adapted phages showed titers against the most recent host
139 strain that were higher than against other strains. For example, K232 (line 1 in Fig. 1) and
140 K2H2 (line 3) showed significantly higher titers against *H. pylori* 26695 (9.6, and 8.2
141 $\log_{10}$ PFU/mL, respectively) than against the other two strains ($p < 0.01$). The same trend
142 was observed in the fourth-stage of phages. K23H3 (line 2) showed a higher titer against
143 3401T (8.6 $\log_{10}$ PFU/mL) than against HPK5 (1.8 $\log_{10}$ PFU/mL) ($p < 0.01$). Similarly,

144 K2H3H (line 4) showed a higher titer against *H. pylori* HPK5 (9.2 $\log_{10}$ PFU/mL) than
145 against 3401T (3.1 $\log_{10}$ PFU/mL, $p < 0.01$).
146 Comparing the adapted phages from different lines, the infectious titers against
147 each of the last host strains were generally similar. For example, K2, K232, and K2H2
148 shared *H. pylori* 26695 as the host strain in the last stage, and all of them showed >8.0
149 $\log_{10}$ PFU/mL against 26695 (8.2–9.6 $\log_{10}$ PFU/mL) but significantly lower titers against
150 other strains (3.1–3.9 $\log_{10}$ PFU/mL). Likewise, K23 and K23H3 showed significantly
151 higher titers against 3401T (8.5–8.6 $\log_{10}$ PFU/mL) than against any other strain. Phages
152 K2H, K23H, and K2H3H also showed significantly higher titers against HPK5 (8.2–9.2
153 $\log_{10}$ PFU/mL) than the others.
154
155 **Genomic analysis of host *H. pylori* strains and adapted phages**
156 SMRT sequencing of two *H. pylori* strains (3401T and HPK5) and three adapted
157 phages (K2, K23, and K2H) was performed to determine the epigenomes of the host
158 strains and adapted phages in the infection flow. Genomic and epigenomic data of *H.*
159 *pylori* 26695 were retrieved from the NCBI RefSeq database (CP003904.1) and a
160 previously published report (37). Complete circular genomes of *H. pylori* 3401T and
161 HPK5 were obtained via *de novo* assembly using HiFi reads (Table S1). The general
162 characteristics of these genomes (e.g., genome size, CDS number, CG content) were
163 similar to those of other *H. pylori* genomes deposited in the NCBI database. The
164 reconstructed *H. pylori* 3401T genome showed >99.99% average nucleotide identity
165 (ANI) to the ancestral strain *H. pylori* 3401 (AP024599.1) (38). Slight differences in
166 sequence most likely arose from genomic mutation during serial subculturing and/or use
167 of different sequencing technologies and bioinformatics software tools. No
168 extrachromosomal content was identified in these strains.
169 Based on functional annotation using REBASE, we predicted 32–36 MTases and
170 16–21 REase genes from the three *H. pylori* genomes (Table S1, S2). The most abundant
171 MTase type was Type II, whereas the other Types I and III were almost compatible. A
172 systematic search of phage-defense systems on the genomes revealed 14, 9, and 14 RM

173 systems from *H. pylori* 26695, 3401T and HPK5, respectively (Table S3). Thus, over half
174 of the detected MTases were orphans. The most abundant modification type was m6A,
175 followed by m5C and m4C. No other systems involved in DNA modification (e.g., BREX
176 (9) and DISARM (10)) were found. In addition to modification-mediated defense systems,
177 6-9 other systems (e.g., AbiL (39) and Dynamins (40, 41)) were identified from the three
178 strains (Table S3).

179 Mapping analysis of KHP30T reads to the original KHP30 phage genome
180 (AB647160.1) (31) identified an approximately 2-kb insertion in all three phages. No
181 single-nucleotide polymorphisms or short indels were found. The insert matched a part
182 of the *H. pylori* 3401 chromosome, indicating the region transferred from the host during
183 serial passaging in the laboratory. The insertion was considered unlikely to significantly
184 affect the general characteristics of the phage (e.g., infection efficiency or host tropism).
185 Indeed, the titration as described above (Fig. 2) was consistent with previous reports (31–
186 33). The KHP30T complete circular genome was reconstructed using HiFi reads from K2
187 phages (Table S1). Based on read mapping analysis, no obvious genomic variations fixed
188 in the population were identified in any of the phages. No MTase and REase genes or
189 phage defense systems were found in the phage genome.

190

191 **Epigenomic analysis of *H. pylori* strains and adapted phages**

192 We successfully identified a number of base modifications in both the *H. pylori*
193 and phage genomes (Fig. 2, Table S4, Fig. S4). From motif predictions, we detected 15
194 and 20 motifs in the *H. pylori* 3401T and HPK5 genomes, respectively, as well as 17
195 motifs in *H. pylori* 26695 retrieved from a previous study (37) (Table S4). Among the
196 motifs, the most abundant modification type was m6A, followed by m4C and m5C. There
197 was a slight discrepancy in modification types of the encoded MTases, possibly
198 underestimated due to the low detection power of m5C modifications by SMRT
199 sequencing. Indeed, the detected m5C motifs showed low modification ratios (<50.0%)
200 in all three *H. pylori* strains. Only two motifs (C**A**<u>T</u>G and G**A**<u>T</u>C, where the bold and
201 underlined characters indicate modified bases and reverse complement of modified bases,

202 respectively) were shared among the three strains, whereas 28 of 39 (72%) motifs were
203 present in either of the three strains, indicating high diversity in the methylated motifs
204 among the strains. This trend is concordant with previous studies that found *H. pylori*
205 strains harbor large numbers of modified motifs with highly divergent combinations
206 among strains (37, 42).

207 Next, we compared the *H. pylori* strains and adapted phages. Overall, methylated
208 motifs were shared between the pairs of *H. pylori* strain and phages that were adapted to
209 the strain (Fig. 3). For example, among the motifs detected from *H. pylori* HPK5 with the
210 exception of m5C motifs, 17 of 19 were highly modified on phage K2H (>68.9% and
211 >63.6% modification ratios of motifs on the host and phage genomes, respectively).
212 Similarly, 12 of 13 motifs were shared between the pair of *H. pylori* 3401T and phage
213 K23 (>73.9% and >41.7%, respectively). Also, 12 of 14 motifs were concordantly
214 methylated between *H. pylori* 26695 and phage K2 (>95.2% and >71.3%, respectively).
215 By contrast, sets of methylated motif were not shared between different combinations of
216 host and phage.

217 Intriguingly, several motifs were identified that were methylated on host
218 genomes but scarcely methylated on adapted phage genomes. For instance, an m6A-type
219 motif G**A**TGG was methylated on the *H. pylori* 3401T genome with a high modification
220 ratio (73.9%), but was absent on the K23 genome. Similarly, motif CCTTG**A** was highly
221 modified in *H. pylori* HPK5 (81.1%) but not in K2H (7.1%). Two motifs, A<u>T</u>TA**A**T and
222 CGR**A**T, were also reported to be methylated with high modification ratios (98.5% and
223 98.9%, respectively) in *H. pylori* 26695 (37), in contrast to K2 (0.0% and 22.6%,
224 respectively).

225

226 **Discussion**

227 *H. pylori* harbors more than 24 MTase genes, some of which are thought to be
228 involved in RM systems (37, 42–45). To better understand the associations of DNA
229 methylation with phage-host interactions, we designed multi-stage infection flows (Fig.
230 1) and analyzed methylomes of three *H. pylori* strains (26695, 3401T and HPK5) and

231 three adapted KHP30T phages (K2, K23, and K2H) with different infection histories. The
232 adapted phages showed high titers against the most recently infected host strain, but much
233 lower titers against the other strains even if previously adapted (Fig. 2). Considering the
234 generation time during cultivation, gene expression disorder or enzymatic inactivation
235 caused by genomic mutations were not expected to significantly affect infection tropism.
236 Indeed, the re-proliferated phages also showed high titers only against the most recently
237 infected host strains (Fig. S5). The three *H. pylori* strains harbored different sets of MTase
238 genes, many of which were located close to the REase genes that comprise the RM
239 systems (Table S1, S2). Based on epigenomic analysis, the adapted phages shared
240 methylated motifs of the last adapted host strain. This observation indicated phage
241 epigenomes were modified by host MTases during infection. Taken together, our work
242 demonstrated that adapted phages acquire DNA methylation by the host, which
243 contributes to escape from the host's RM systems and increased infection efficiency, as
244 has long been assumed (46). Nonetheless, this is the first study to report direct
245 observations of epigenomic changes in the phage genome during infection (Fig. S4).

246 Overall the methylated motifs were shared between the adapted phage and host,
247 but some exceptions were found. Specifically, several motifs were modified in the host
248 genome but not in the adapted phage (Fig. 3). These exceptions may, in part at least, be
249 explained by phase variation found in several RM systems from *H. pylori* strains (Fig.
250 S3). Phase variation, a mechanism of random and reversible switching of gene expression,
251 generates transcriptional, translational, and/or phenotypic variation in a bacterial
252 population (47). Bacterial MTases associated with RM systems are phase-variable,
253 resulting in heterogeneous cells with active or inactive RM systems within the clonal
254 population (48). Consequently, phages prefer to infect RM system-reduced cells, and the
255 majority of phage epigenome is thus catalyzed by the set of MTases encoded by such
256 hosts. One of the key signatures that regulates phase variation is a simple sequence repeat
257 (SSR) inside or upstream of the gene; in the former case, phase-variable ON/OFF
258 switching occurs resulting in reversible changes in the number of SSRs (48–52). Here,
259 we found several phase-variable regulons (phasevarions) associated with RM system

genes in the three *H. pylori* genomes (Fig. S3, Supplemental text). Additional experimental evaluation at single-cell resolution would be required to better understand the relationship between phase variation and phage infection (e.g., a combination of immunofluorescence imaging for measurement of phase variated proteins (53) and fluorescence *in situ* hybridization for detecting infected phages). Moreover, bioinformatics needs to be improved because current modification detection tools are not designed to consider phase-variation epigenomes. Instead, these tools call statistically-certain modifications within a population in binary scale. Another possible explanation for unshared methylated motifs is that the phage have anti-RM systems that block the host MTase activity. For example, proteins DarA and DarB from P1 phage protect recognition sites on their genome from host RM systems (54, 55), and Ocr of T7 phage mimics phage DNA structure to block the DNA-binding groove of Type I REases/MTases (56). No genes associated with known anti-RM systems listed in a previous review (57) were found in the KHP30T genome.

There are several limitations to this study. First, we have not experimentally confirmed the activities and specificity of the MTases and REases. Thus, it is still unclear which RM systems are effective for phage defense as well as the identity of MTases responsible for the modified motifs. Second, while SMRT sequencing technology efficiently identifies m6A and m4C modifications (37) other types of modification exist in nature. Among these methylations, m5C modification is one of the most widespread modifications following m6A and m4C. In total, five m5C motifs were detected in the three *H. pylori* strains (Table S4). All of them showed low modification ratios (Fig. 3, Table S4), presumably due to the low detection power of the modification type using current SMRT technology. In addition to methylation, other epigenetic modifications, such as phosphorothioate modification, have recently been reported to play a significant role in phage defense (58). To better understand epigenomic functions, further methodological developments to measure a wide variety of DNA modifications are required. Third, although HiFi reads are highly accurate (>99.9%), sequencing of homopolymer regions remains challenging (59–61). Thus, it is still difficult to estimate

289 tract number diversity. Nonetheless, because of high genome coverages (Table S1), tracts
290 associated with RM genes (Fig. S3) likely reflect the dominant state of the actual phase
291 variation within a population.

292 Defense systems are involved in an arms race between phages and hosts (62).
293 Thus, epigenomic systems greatly impact eco-evolution and promote microbial
294 diversification (63, 64). Our data showed that the phage epigenome was changed by its
295 host bacteria during infection, resulting in the reinforcement of phage infection ability
296 against the host (Figs. 2, 3). To counter the epigenomic synchronization of phages and to
297 avoid the extinction of the entire host population by phage prevalence, some prokaryotes
298 change their sets of phage-defense systems heterogeneously. For example, many species
299 of gut bacteria, such as *Bacteroides fragilis* and *H. pylori*, showed strain-level variations
300 in gene sets involved in phage defense systems including MTases (65–67). However,
301 because gene acquisition and deletion relies on genomic events, such as horizontal gene
302 transfer and recombination, this occurs at low frequently. By contrast, a more dynamic
303 strategy involves phase variation for phage prevalence prevention in the community. For
304 example, in *Vibrio cholerae* phase variation modulates the expression of
305 lipopolysaccharide O1 antigen to escape predation by an O1-specific phage (68). In the
306 case of *H. pylori*, inter-strain variation in methylomes caused by MTase phase variation
307 have been reported (42, 43). Thus, antagonistic co-evolution within prokaryotes and
308 phages associated with epigenetic changes is of interest in understanding a wide range of
309 microbial ecosystems.

310 Our results are also emerged an attention to the potential application of phage
311 therapy. The gastrointestinal microbiome involves a complex set of interactions that are
312 closely related to human physiology, such as the metabolic, immune, and neuroendocrine
313 systems (69). *H. pylori* is one of the most common human gastrointestinal pathogens that
314 colonizes over half of the world's population. *H. pylori* infection is a risk factor for gastric
315 cancer, which is the second leading cause of cancer-related deaths (70–72). Given the
316 prevalence of antibiotic-resistant *H. pylori*, development of alternative treatment
317 approaches is crucial (73, 74). One promising approach is the utilization of lytic phages

318 as a self-amplifying drug to specifically kill susceptible bacteria (75, 76). Phages have
319 favorable characteristics such as host-specificity, self-amplification, biofilm degradation,
320 and low toxicity to human (77, 78). Indeed, phage therapy is expected to contribute to the
321 treatment of a wide range of infectious diseases in human and plants (79–82). However,
322 the strategy is not effective against prokaryotes that resist phage infection. Controlling
323 DNA modifications in the phage genome in advance of their therapeutic application
324 would be needed to avoid degradation by host modification-mediated defense systems
325 such as RM system. One possible approach entails the preparation of a cocktail of adapted
326 phages whose epigenomes are diversified using variable sets of MTases. The concept of
327 the phage cocktail has already been proposed and experimentally evaluated using
328 *Escherichia coli* O157:H7 and *Klebsiella pneumoniae* (83, 84). The preparation of a set
329 of adapted phages with different epigenomes covering all possible motifs specified by
330 host RM systems would be technically demanding. Nonetheless, such a cocktail would
331 increase the probability of overcoming the host's defense systems. For example, the
332 multi-stage infection flow (Fig. 1) could be used for the adaptive evolution of phages to
333 improve their endogenous ability to resist stress caused by temperature changes or
334 exposure to UV radiation (85–87). Indeed, this infection approach was applied to generate
335 pre-adapting phages under the host-phage co-evolutionary system (i.e., phage training)
336 (88, 89). Further research to understand the mechanism of phage adaptation and to
337 evaluate the therapeutic potential of adapted phages would contribute to the good design
338 of phage cocktails aiming for medical and industrial applications.
339
340 **Conclusions**
341 In this study, our data provides evidence that a phage passed through the host
342 RM system acquired methylation modifications mediated by host-encoded MTases
343 during infection. The adapted phage showed significantly higher titer against the last
344 infected host strain. This observation likely arises due to the neutralization of the host RM
345 system by the acquired modifications. Our results help elucidate the DNA methylation-
346 mediated phage–host interactions that significantly impact on microbial ecology in a wide

347 range of environments.

348

349

350 **Materials and Methods**

351 **Culture conditions of *H. pylori* and phages**

352 *H. pylori* 26695, 3401T (derived from *H. pylori* 3401) and HPK5 were routinely
353 cultured on BEV plates (Brucella broth [Becton Dickinson, Cockeysville, MD, USA]
354 supplemented with 1.5% agar, 10% heat-inactivated equine serum [Hyclone Laboratories,
355 South Logan, UT, USA], and 10 μg/mL vancomycin) at 37°C under microaerobic
356 conditions (10% CO_2). A preculture of *H. pylori* was prepared by incubating in 5 mL of
357 BEV broth at 37°C under microaerobic conditions with shaking (200 rpm of reciprocating
358 shaking with an EYEKA multi-shaker; Tokyo Rikakikai, Tokyo, Japan) for 20 h.

359 Phage KHP30T, working stock of KHP30 was prepared from a filtered
360 supernatant of *H. pylori* 3401 after inoculation of KHP30 as described previously (31).
361 Phage stocks were stored at 4°C. Nine adapted phage cultures were prepared by using
362 KHP30T to infect three *H. pylori* strains (26695, 3401T, and/or HPK5) in defined
363 sequential steps (Fig. 1). Detailed procedures for phage adaptation are described in
364 Supplemental text.

365

366 **Titration of adapted phages**

367 The infectious titers of nine adapted phages (K2, K23, K232, K23H, K23H3,
368 K2H, K2H2, K2H3, K2H3H) and three re-proliferated phages (K2, K23, K2H cultured
369 at large-scale; see Supplemental text) were measured by plaque assay (32). In brief, 100
370 μL of serial 10-fold diluted adapted phages (Fig. S1 right) and 500 μL of *H. pylori*
371 preculture (approximately 1×10^8 CFU/mL) were co-cultured on double-layered plates.
372 Plaques were counted after incubation at 37°C under microaerobic conditions for 3 days.
373 Each experiment was carried out in three independent biological replicates (n = 3) and
374 each biological replicate contained two technical replicates. To test the differences in
375 phage titers, Tukey-Kramer test was performed using 'multcomp' R package version 1.4-
376 20.

377

378 **DNA extraction and SMRT sequencing**

379 Genomic DNAs of *H. pylori* 3401T and HPK5 were extracted using QIAGEN
380 Genomic-tips 100/G (QIAGEN, Hilden, Germany) according to the manufacturer's
381 instructions. For SMRT sequencing, library preparation and high-fidelity (HiFi)
382 sequencing using the PacBio Sequel II system (Pacific Biosciences, Menlo Park, CA,
383 USA) were performed by Macrogen Japan (Tokyo, Japan).

384 Genome DNAs of three adapted phages (K2H, K2, K23) were prepared using
385 the phenol-chloroform extraction method after large-scale cultivation and particle
386 purification (see Supplemental text). For K2H, the extracted genomic DNA was sheared
387 to 10 kb for SMRTbell library preparation and subjected to SMRT sequencing in
388 continuous long read (CLR) mode using the PacBio Sequel system (Pacific Biosciences).
389 For K2 and K23, DNA were shared to 10-15 kb length for SMRTbell library preparation
390 and sequenced in circular consensus sequencing (CCS) mode using PacBio Sequel II
391 system (Pacific Biosciences). All library preparation and sequencing for the phages were
392 performed by Azenta (South Plainfield, NJ, USA).

393

394 **Bioinformatics**

395 For *H. pylori* 3401T and HPK5, HiFi reads were converted to add conventional
396 kinetic information using ccs-kinetics-bystrandify script, provided by PacBio. HiFi reads
397 were *de novo* assembled using Hifiasm (90) with the '-l0' option. Each circular
398 chromosomal genome was then manually retrieved. To reduce calculation times for
399 modification identification, low complexity regions were masked using komplexity
400 (https://github.com/eclarke/komplexity) with '--mask --threshold 0.65' options. HiFi
401 reads were mapped to the masked genomes using pbmm2, an official wrapper software
402 for minimap2 (91), to calculate interpulse duration ratios. Modification detection and
403 motif prediction were performed using ipdSummary a and MotifMaker, respectively
404 (SMRT Link package v12.0 with default settings). Considering the detection power of
405 modified nucleotides by SMRT sequencing, m4C and m6A motifs with scores >100000

406 and all m5C motifs were retrieved as candidate methylated motifs. Motifs with
407 ambiguous sequences were manually curated. For example, TCG**A**VV (where V =
408 A/C/G) was detected in *H. pylori* 3401T, but the spurious partial sequence VV was likely
409 due to incomplete detection of the motif, and probably represents the palindrome TCG**A**.
410 Data on methylated motifs in *H. pylori* 26695 were retrieved from a previous study (37).
411 For the phage genome sequenced in CCS mode (K2 and K23), subreads
412 containing at least three full-pass subreads on each polymerase read and with >99%
413 average base-call accuracy were retained as HiFi reads using the standard PacBio SMRT
414 software package with default settings. For downstream epigenomic analysis, HiFi reads
415 were converted to add conventional kinetic information. HiFi reads from K2 were then
416 *de novo* assembled using canu (92) with '-pacbio-hifi genomeSize=30k' options, and one
417 chromosomal genome was retrieved after manual curation. For comparative genomic
418 analysis, a reference KHP30 genome (AB647160.1) was retrieved from the NCBI RefSeq
419 Database, and subreads (K2H) and HiFi reads (K2 and K23) were mapped on the
420 reference genome using pbmm2 with subreads or HiFi read mode, respectively. For
421 epigenomic analysis, subreads and HiFi reads from each phage were mapped to the
422 assembled KHP30T genome as described above. Nucleotide modifications were
423 predicted using ipdSummary a and MotifMaker from SMRT Link packages v10.2 and
424 v12.0 for PacBio Sequel and Sequel II data, respectively, according to the supported
425 systems of each software version, with the default settings. The algorithm used by
426 MotifMaker employs a statistical test for motif identification and was therefore not
427 applicable to small phage genomes, in which insufficient number of motif sequences for
428 de novo identification of modified motifs (26). Consequently, we focused on the host
429 genomes for motif prediction.
430 CDSs with >33 aa length in each genome were predicted using Prodigal (93)
431 with default settings or with '-meta' option for *H. pylori* and phage genomes, respectively.
432 Genes encoding MTases, REases, and DNA sequence-recognition proteins (S subunits)
433 were identified using DIAMOND (94). Sequences were compared against an
434 experimentally confirmed gold-standard dataset from REBASE (95) (downloaded on 1st

March 2024), with a cutoff e-value of ≤1E-5. REBASE was used to retrieve sequence specificity for each MTase and REase. Phage defense systems were predicted using PADLOC (96). ANI was calculated using FastANI (97). Circos plots were generated using 'interacCircos' R package (98). Homopolymers with more than nine repeat numbers and located inside or less than 100 bp upstream of RM system genes were retrieved as SSRs associated with the RM system.

Acknowledgments

The authors thankfully acknowledge Kazuhiro Hanazaki (Kochi University Hospital) for the financial support. The authors are greatful to Waka Ishida and Yusaku Funaoka for experimental support, and to Daichi Morimoto for helpful comments on this work. The experiments were conducted at the Division of Biological Research, Science Research Center, Kochi University. Computations were partially performed on the supercomputer system at the Institute for Chemical Research, Kyoto University, and the NIG supercomputer system at ROIS National Institute of Genetics, and the Data Analysis and the Earth Simulator systems at JAMSTEC.

Author contributions

M.T. designed the study, acquired funding, performed the experiments, and drafted the manuscript. S.H. designed the study, performed the bioinformatics analyses, and wrote the manuscript. Y.M., R.S., and T.U. performed the experiments. H.M. acquired funding and provided resources. S.S., K.N., and H.T. supervised the project. S.M. conceived the original idea, acquired funding, and supervised the project. All authors have read and approved the final manuscript.

Data availability

The assembled genomes were deposited in DDBJ/ENA/GenBank (Table S1). All data are registered under BioProject ID PRJDB17787 [https://ddbj.nig.ac.jp/resource/bioproject/PRJDB17787].

Funding

This study was supported by JSPS KAKENHI (grant numbers JP20K15582 and JP22K08875), ACT-X, Japan Science and Technology Agency (grant numbers JPMJAX21BD and JPMJAX22BK), and the budget of Kochi University Hospital (Japan).

470 **Figure legends**

471 **Fig. 1 Overview of multi-stage infection flow.** Nine KHP30T phages were prepared by
472 adapting to three strains of *H. pylori* (26695, 3401T, HPK5) through four infection stages
473 and four lines. Details of the adaptation procedure are provided in the Supplemental text
474 and Fig. S1.

475

476 **Fig. 2 Infectious titer of adapted KHP30T.** Orange, blue, and green bars represent
477 KHP30T titers against *H. pylori* 26695, 3401T, and HPK5, respectively. Error bars
478 represent standard deviation ($n = 3$).

479

480 **Fig. 3 Methylomes of adapted phages and *H. pylori* strains.** Methylated motifs were
481 predicted from the three *H. pylori* strains. Motifs are shown separately according to
482 methylation type. Phages and *H. pylori* strains are colored in red and black, respectively,
483 in the bottom text. Text on the left side indicates the methylated motifs with methylated
484 nucleotide position and methylation type. The top dendrogram was calculated using
485 Euclidean distance and Ward method. For *H. pylori* 26695, methylated motifs and ratios
486 were retrieved from the previous study reported by Krebes et al. (2014), and gray cells
487 indicate motifs for which no data are available. Some motifs showed comparatively high
488 modification ratios due to motif overlap. For example, the modification ratio of CGR**A**T
489 (R=A/G) in *H. pylori* 3401T is explained by motif overlapping with CGR**A**, which was
490 detected from epigenomic analysis of the strain. In addition, CGW**A**G (W=A/T) in *H.*
491 *pylori* 3401T partly overlapped with CGR**A**, i.e., CGA**A**G. A motif G**A**GG in *H. pylori*
492 HPK5 also overlapped with the detected G**A**GGA from the strain, and in contrast,
493 G**A**GGA in K2 overlap with G**A**GG reported from *H. pylori* 26695 previously. Among
494 all seven CCGC**A**T sites in K23, two and one overlapped with other motifs C**A**TG (i.e.,
495 CCGC**A**TG) and **A**TCC (i.e., CCGC**A**TCC), respectively. Hence, CCGC**A**T showed a
496 comparatively higher modification ratio in K23.

497

498 **Fig. S1 Overview of preparation procedure for adapted phages.**

499

500 **Fig. S2 Tukey-Kramer pairwise comparisons of phage titers.** Corresponding titers are
501 shown in Fig. 2. Combination of phage and host strain are indicated as 'adapted phage':
502 'initial of host strain' format in the x-axis: for example, 'K2:2' means a titer of K2 against
503 *H. pylori* 26695. Solid black bar within each box represents median. Upper alphabet

summarizes the results of the Tukey-Kramer test; letters denote significant differences ($p < 0.01$) in mean titers with groups a > b > c > d > e > f.

Fig. S3 Genetic organization of RM system genes associated with SSRs. Homopolymeric tracts inside or upstream of RM genes were specified as SSRs. RM gene types are indicated by color and text inside to each CDS. CDSs not assigned to RM system genes are colored in gray.

Fig. S4 Methylomes of adapted phages. Circos plot showing the distribution of DNA methylation. Orange, blue, and red bars represent m4C, m5C, and m6A modifications, respectively. K2 and K23 were sequenced using PacBio Sequel II in CCS mode, whereas K2H was sequenced using PacBio Sequel in CLR mode.

Fig. S5 Infectious titer of re-proliferated phages. (a) Orange, blue, and green bars represent titer of re-proliferated KHP30T phages to *H. pylori* 26695, 3401T, and HPK5, respectively. Error bars indicate standard deviation ($n = 3$). (b) Tukey-Kramer pairwise comparisons of re-proliferated phage titers. Phage and host combinations are indicated in the same format as Fig. S2. Infectious titer of the 'Original phages' is derived from Fig. 2. Solid black bar within each box represents median. Upper alphabet summarizes the results of the Tukey-Kramer test; letters denote significant differences ($p < 0.01$) in mean titers with groups a > b > c > d > e > f.

Supplemental tables

Table S1 Descriptions and statistics of *H. pylori* strains and KHP30T phages.

Table S2 Detected RM system genes in *H. pylori* strains.

Table S3 Predicted phage defense systems in *H. pylori* strains.

Table S4. Methylated motifs predicted from *H. pylori* strains.

534 **References**

535 1. Struck A-W, Thompson ML, Wong LS, Micklefield J. 2012. S-adenosyl-methionine-
536 dependent methyltransferases: highly versatile enzymes in biocatalysis, biosynthesis
537 and other biotechnological applications. Chembiochem 13:2642–2655.
538 2. Weigele P, Raleigh EA. 2016. Biosynthesis and function of modified bases in bacteria
539 and their viruses. Chem Rev 116:12655–12687.
540 3. Seong HJ, Han S-W, Sul WJ. 2021. Prokaryotic DNA methylation and its functional
541 roles. J Microbiol 59:242–248.
542 4. Labrie SJ, Samson JE, Moineau S. 2010. Bacteriophage resistance mechanisms. Nat
543 Rev Microbiol 8:317–327.
544 5. Ando T, Ishiguro K, Watanabe O, Miyake N, Kato T, Hibi S, Mimura S, Nakamura
545 M, Miyahara R, Ohmiya N, Niwa Y, Goto H. 2010. Restriction-modification systems
546 may be associated with *Helicobacter pylori* virulence. J Gastroenterol Hepatol 25
547 Suppl 1:S95-8.
548 6. Arber W. 1974. DNA modification and restriction. Prog Nucleic Acid Res Mol Biol
549 14:1–37.
550 7. Ershova AS, Rusinov IS, Spirin SA, Karyagina AS, Alexeevski AV. 2015. Role of
551 restriction-modification systems in prokaryotic evolution and ecology. Biochemistry
552 80:1373–1386.
553 8. Mruk I, Kobayashi I. 2014. To be or not to be: regulation of restriction-modification
554 systems and other toxin-antitoxin systems. Nucleic Acids Res 42:70–86.
555 9. Goldfarb T, Sberro H, Weinstock E, Cohen O, Doron S, Charpak-Amikam Y, Afik S,
556 Ofir G, Sorek R. 2015. BREX is a novel phage resistance system widespread in
557 microbial genomes. EMBO J 34:169–183.
558 10. Ofir G, Melamed S, Sberro H, Mukamel Z, Silverman S, Yaakov G, Doron S, Sorek
559 R. 2017. DISARM is a widespread bacterial defence system with broad anti-phage
560 activities. Nat Microbiol 3:90–98.
561 11. Zhou X, Wang J, Herrmann J, Moerner WE, Shapiro L. 2019. Asymmetric division
562 yields progeny cells with distinct modes of regulating cell cycle-dependent
563 chromosome methylation. Proc Natl Acad Sci U S A 116:15661–15670.
564 12. Kozdon JB, Melfi MD, Luong K, Clark TA, Boitano M, Wang S, Zhou B, Gonzalez
565 D, Collier J, Turner SW, Korlach J, Shapiro L, McAdams HH. 2013. Global
566 methylation state at base-pair resolution of the *Caulobacter* genome throughout the
567 cell cycle. Proc Natl Acad Sci U S A 110:E4658-67.
568 13. Vandenbussche I, Sass A, Pinto-Carbó M, Mannweiler O, Eberl L, Coenye T. 2020.
569 DNA methylation epigenetically regulates gene expression in *Burkholderia*

570 *cenocepacia* and controls biofilm formation, cell aggregation, and motility. mSphere
571 5.
572 14. Oliveira PH, Ribis JW, Garrett EM, Trzilova D, Kim A, Sekulovic O, Mead EA, Pak
573 T, Zhu S, Deikus G, Touchon M, Lewis-Sandari M, Beckford C, Zeitouni NE, Altman
574 DR, Webster E, Oussenko I, Bunyavanich S, Aggarwal AK, Bashir A, Patel G,
575 Wallach F, Hamula C, Huprikar S, Schadt EE, Sebra R, van Bakel H, Kasarskis A,
576 Tamayo R, Shen A, Fang G. 2020. Epigenomic characterization of *Clostridioides*
577 *difficile* finds a conserved DNA methyltransferase that mediates sporulation and
578 pathogenesis. Nat Microbiol 5:166–180.
579 15. Nye TM, Jacob KM, Holley EK, Nevarez JM, Dawid S, Simmons LA, Watson ME
580 Jr. 2019. DNA methylation from a Type I restriction modification system influences
581 gene expression and virulence in *Streptococcus pyogenes*. PLoS Pathog 15:e1007841.
582 16. Mannweiler O, Pinto-Carbó M, Lardi M, Agnoli K, Eberl L. 2021. Investigation of
583 Burkholderia cepacia complex methylomes via single-molecule, real-time
584 sequencing and mutant analysis. J Bacteriol 203:e0068320.
585 17. Srikhanta YN, Fox KL, Jennings MP. 2010. The phasevarion: phase variation of type
586 III DNA methyltransferases controls coordinated switching in multiple genes. Nat
587 Rev Microbiol 8:196–206.
588 18. Furuta Y, Kobayashi I. 2012. Mobility of DNA sequence recognition domains in
589 DNA methyltransferases suggests epigenetics-driven adaptive evolution. Mob Genet
590 Elements 2:292–296.
591 19. Sánchez-Romero MA, Casadesús J. 2020. The bacterial epigenome. Nat Rev
592 Microbiol 18:7–20.
593 20. Friman V-P, Soanes-Brown D, Sierocinski P, Molin S, Johansen HK, Merabishvili M,
594 Pirnay J-P, De Vos D, Buckling A. 2016. Pre-adapting parasitic phages to a pathogen
595 leads to increased pathogen clearance and lowered resistance evolution with
596 *Pseudomonas aeruginosa* cystic fibrosis bacterial isolates. J Evol Biol 29:188–198.
597 21. Rohde C, Resch G, Pirnay J-P, Blasdel B, Debarbieux L, Gelman D, Górski A, Hazan
598 R, Huys I, Kakabadze E, Łobocka M, Maestri A, Almeida G, Makalatia K, Malik D,
599 Mašlaňová I, Merabishvili M, Pantucek R, Rose T, Štveráková D, Van Raemdonck
600 H, Verbeken G, Chanishvili N. 2018. Expert opinion on three phage therapy related
601 topics: Bacterial phage resistance, phage training and prophages in bacterial
602 production strains. Viruses 10:178.
603 22. Krüger DH, Bickle TA. 1983. Bacteriophage survival: multiple mechanisms for
604 avoiding the deoxyribonucleic acid restriction systems of their hosts. Microbiol Rev
605 47:345–360.

606 23. Coy SR, Gann ER, Papoulis SE, Holder ME, Ajami NJ, Petrosino JF, Zinser ER, Van
607 Etten JL, Wilhelm SW. 2020. SMRT sequencing of Paramecium bursaria chlorella
608 virus-1 reveals diverse methylation stability in adenines targeted by restriction
609 modification systems. Front Microbiol 11:887.
610 24. Forde BM, McAllister LJ, Paton JC, Paton AW, Beatson SA. 2019. SMRT
611 sequencing reveals differential patterns of methylation in two O111:H- STEC
612 isolates from a hemolytic uremic syndrome outbreak in Australia. Sci Rep 9:9436.
613 25. Hiraoka S, Okazaki Y, Anda M, Toyoda A, Nakano S-I, Iwasaki W. 2019.
614 Metaepigenomic analysis reveals the unexplored diversity of DNA methylation in an
615 environmental prokaryotic community. Nat Commun 10:159.
616 26. Hiraoka S, Sumida T, Hirai M, Toyoda A, Kawagucci S, Yokokawa T, Nunoura T.
617 2022. Diverse DNA modification in marine prokaryotic and viral communities.
618 Nucleic Acids Res 50:1531–1550.
619 27. Jeudy S, Rigou S, Alempic J-M, Claverie J-M, Abergel C, Legendre M. 2020. The
620 DNA methylation landscape of giant viruses. Nat Commun 11:2657.
621 28. Murray IA, Clark TA, Morgan RD, Boitano M, Anton BP, Luong K, Fomenkov A,
622 Turner SW, Korlach J, Roberts RJ. 2012. The methylomes of six bacteria. Nucleic
623 Acids Res 40:11450–11462.
624 29. Murphy J, Klumpp J, Mahony J, O'Connell-Motherway M, Nauta A, van Sinderen
625 D. 2014. Methyltransferases acquired by lactococcal 936-type phage provide
626 protection against restriction endonuclease activity. BMC Genomics 15:831.
627 30. Sun C, Chen J, Jin M, Zhao X, Li Y, Dong Y, Gao N, Liu Z, Bork P, Zhao X-M, Chen
628 W-H. 2023. Long-read sequencing reveals extensive DNA methylations in human
629 gut phagenome contributed by prevalently phage-encoded methyltransferases. Adv
630 Sci (Weinh) 10:e2302159.
631 31. Uchiyama J, Takeuchi H, Kato S-I, Takemura-Uchiyama I, Ujihara T, Daibata M,
632 Matsuzaki S. 2012. Complete genome sequences of two *Helicobacter pylori*
633 bacteriophages isolated from Japanese patients. J Virol 86:11400–11401.
634 32. Uchiyama J, Takeuchi H, Kato S-I, Gamoh K, Takemura-Uchiyama I, Ujihara T,
635 Daibata M, Matsuzaki S. 2013. Characterization of *Helicobacter pylori*
636 bacteriophage KHP30. Appl Environ Microbiol 79:3176–3184.
637 33. Kamiya R, Uchiyama J, Matsuzaki S, Murata K, Iwasaki K, Miyazaki N. 2022. Acid-
638 stable capsid structure of *Helicobacter pylori* bacteriophage KHP30 by single-
639 particle cryoelectron microscopy. Structure 30:300-312.e3.
640 34. Ando T, Xu Q, Torres M, Kusugami K, Israel DA, Blaser MJ. 2000. Restriction-
641 modification system differences in *Helicobacter pylori* are a barrier to interstrain

642 plasmid transfer. Mol Microbiol 37:1052–1065.
643 35. Alm RA, Ling LS, Moir DT, King BL, Brown ED, Doig PC, Smith DR, Noonan B,
644 Guild BC, deJonge BL, Carmel G, Tummino PJ, Caruso A, Uria-Nickelsen M, Mills
645 DM, Ives C, Gibson R, Merberg D, Mills SD, Jiang Q, Taylor DE, Vovis GF, Trust
646 TJ. 1999. Genomic-sequence comparison of two unrelated isolates of the human
647 gastric pathogen *Helicobacter pylori*. Nature 397:176–180.
648 36. Bubendorfer S, Krebes J, Yang I, Hage E, Schulz TF, Bahlawane C, Didelot X,
649 Suerbaum S. 2016. Genome-wide analysis of chromosomal import patterns after
650 natural transformation of *Helicobacter pylori*. Nat Commun 7:11995.
651 37. Krebes J, Morgan RD, Bunk B, Spröer C, Luong K, Parusel R, Anton BP, König C,
652 Josenhans C, Overmann J, Roberts RJ, Korlach J, Suerbaum S. 2014. The complex
653 methylome of the human gastric pathogen *Helicobacter pylori*. Nucleic Acids Res
654 42:2415–2432.
655 38. Takahashi M, Matsumoto Y, Ujihara T, Maeda H, Hanazaki K, Nagasaki K, Takeuchi
656 H, Matsuzaki S. 2021. Complete genome sequence of *Helicobacter pylori* strain
657 3401, a suitable host for bacteriophages KHP30 and KHP40. Microbiol Resour
658 Announc 10:e0064721.
659 39. Deng Y-M, Liu C-Q, W. Dunn N. 1999. Genetic organization and functional analysis
660 of a novel phage abortive infection system, AbiL, from *Lactococcus lactis*. J
661 Biotechnol 67:135–149.
662 40. Millman A, Melamed S, Leavitt A, Doron S, Bernheim A, Hör J, Garb J, Bechon N,
663 Brandis A, Lopatina A, Ofir G, Hochhauser D, Stokar-Avihail A, Tal N, Sharir S,
664 Voichek M, Erez Z, Ferrer JLM, Dar D, Kacen A, Amitai G, Sorek R. 2022. An
665 expanded arsenal of immune systems that protect bacteria from phages. Cell Host
666 Microbe 30:1556-1569.e5.
667 41. Guo L, Sattler L, Shafqat S, Graumann PL, Bramkamp M. 2022. A bacterial
668 dynamin-like protein confers a novel phage resistance strategy on the population
669 level in *Bacillus subtilis*. MBio 13.
670 42. Furuta Y, Namba-Fukuyo H, Shibata TF, Nishiyama T, Shigenobu S, Suzuki Y,
671 Sugano S, Hasebe M, Kobayashi I. 2014. Methylome diversification through changes
672 in DNA methyltransferase sequence specificity. PLoS Genet 10:e1004272.
673 43. Nell S, Estibariz I, Krebes J, Bunk B, Graham DY, Overmann J, Song Y, Spröer C,
674 Yang I, Wex T, Korlach J, Malfertheiner P, Suerbaum S. 2018. Genome and
675 methylome variation in *Helicobacter pylori* with a *cag* pathogenicity island during
676 early stages of human infection. Gastroenterology 154:612-623.e7.
677 44. Estibariz I, Overmann A, Ailloud F, Krebes J, Josenhans C, Suerbaum S. 2019. The

core genome m5C methyltransferase JHP1050 (M.Hpy99III) plays an important role in orchestrating gene expression in *Helicobacter pylori*. Nucleic Acids Res 47:2336–2348.

45. Vasu K, Nagaraja V. 2013. Diverse functions of restriction-modification systems in addition to cellular defense. Microbiol Mol Biol Rev 77:53−72.
46. Isaev AB, Musharova OS, Severinov KV. 2021. Microbial arsenal of antiviral defenses - Part I. Biochemistry 86:319–337.
47. de Vries N, Duinsbergen D, Kuipers EJ, Pot RGJ, Wiesenekker P, Penn CW, van Vliet AHM, Vandenbroucke-Grauls CMJE, Kusters JG. 2002. Transcriptional phase variation of a type III restriction-modification system in *Helicobacter pylori*. J Bacteriol 184:6615–6623.
48. Atack JM, Tan A, Bakaletz LO, Jennings MP, Seib KL. 2018. Phasevarions of bacterial pathogens: methylomics sheds new light on old enemies. Trends Microbiol 26:715–726.
49. Gor V, Ohniwa RL, Morikawa K. 2021. No change, no life? What we know about phase variation in *Staphylococcus aureus*. Microorganisms 9:244.
50. Nahar N, Tram G, Jen FE-C, Phillips ZN, Weinert LA, Bossé JT, Jabbari JS, Gouil Q, Du MRM, Ritchie ME, Bowden R, Langford PR, Tucker AW, Jennings MP, Turni C, Blackall PJ, Atack JM. 2023. *Actinobacillus pleuropneumoniae* encodes multiple phase-variable DNA methyltransferases that control distinct phasevarions. Nucleic Acids Res 51:3240–3260.
51. Moxon R, Bayliss C, Hood D. 2006. Bacterial contingency loci: the role of simple sequence DNA repeats in bacterial adaptation. Annu Rev Genet 40:307–333.
52. Bayliss CD. 2009. Determinants of phase variation rate and the fitness implications of differing rates for bacterial pathogens and commensals. FEMS Microbiol Rev 33:504–520.
53. Ben-Assa N, Coyne MJ, Fomenkov A, Livny J, Robins WP, Muniesa M, Carey V, Carasso S, Gefen T, Jofre J, Roberts RJ, Comstock LE, Geva-Zatorsky N. 2020. Analysis of a phase-variable restriction modification system of the human gut symbiont *Bacteroides fragilis*. Nucleic Acids Res 48:11040–11053.
54. Iida S, Streiff MB, Bickle TA, Arber W. 1987. Two DNA antirestriction systems of bacteriophage P1, *darA*, and *darB*: characterization of *darA*- phages. Virology 157:156–166.
55. Teklemariam AD, Al-Hindi RR, Qadri I, Alharbi MG, Ramadan WS, Ayubu J, Al-Hejin AM, Hakim RF, Hakim FF, Hakim RF, Alseraihi LI, Alamri T, Harakeh S. 2023.

The battle between bacteria and bacteriophages: a conundrum to their immune system. Antibiotics (Basel) 12.

56. Roberts GA, Stephanou AS, Kanwar N, Dawson A, Cooper LP, Chen K, Nutley M, Cooper A, Blakely GW, Dryden DTF. 2012. Exploring the DNA mimicry of the Ocr protein of phage T7. Nucleic Acids Res 40:8129–8143.
57. Samson JE, Magadán AH, Sabri M, Moineau S. 2013. Revenge of the phages: defeating bacterial defences. Nat Rev Microbiol 11:675–687.
58. Jiang S, Chen K, Wang Y, Zhang Y, Tang Y, Huang W, Xiong X, Chen S, Chen C, Wang L. 2023. A DNA phosphorothioation-based Dnd defense system provides resistance against various phages and is compatible with the Ssp defense system. MBio 14:e0093323.
59. Hebert PDN, Braukmann TWA, Prosser SWJ, Ratnasingham S, deWaard JR, Ivanova NV, Janzen DH, Hallwachs W, Naik S, Sones JE, Zakharov EV. 2018. A Sequel to Sanger: amplicon sequencing that scales. BMC Genomics 19.
60. Wenger AM, Peluso P, Rowell WJ, Chang P-C, Hall RJ, Concepcion GT, Ebler J, Fungtammasan A, Kolesnikov A, Olson ND, Töpfer A, Alonge M, Mahmoud M, Qian Y, Chin C-S, Phillippy AM, Schatz MC, Myers G, DePristo MA, Ruan J, Marschall T, Sedlazeck FJ, Zook JM, Li H, Koren S, Carroll A, Rank DR, Hunkapiller MW. 2019. Accurate circular consensus long-read sequencing improves variant detection and assembly of a human genome. Nat Biotechnol 37:1155–1162.
61. Mc Cartney AM, Shafin K, Alonge M, Bzikadze AV, Formenti G, Fungtammasan A, Howe K, Jain C, Koren S, Logsdon GA, Miga KH, Mikheenko A, Paten B, Shumate A, Soto DC, Sović I, Wood JMD, Zook JM, Phillippy AM, Rhie A. 2022. Chasing perfection: validation and polishing strategies for telomere-to-telomere genome assemblies. Nat Methods 19:687–695.
62. Hampton HG, Watson BNJ, Fineran PC. 2020. The arms race between bacteria and their phage foes. Nature 577:327–336.
63. Scanlan PD. 2017. Bacteria-bacteriophage coevolution in the human gut: implications for microbial diversity and functionality. Trends Microbiol 25:614–623.
64. Dimitriu T, Szczelkun MD, Westra ER. 2020. Evolutionary ecology and interplay of prokaryotic innate and adaptive immune systems. Curr Biol 30:R1189–R1202.
65. O'Connell Motherway M, Zomer A, Leahy SC, Reunanen J, Bottacini F, Claesson MJ, O'Brien F, Flynn K, Casey PG, Munoz JAM, Kearney B, Houston AM, O'Mahony C, Higgins DG, Shanahan F, Palva A, de Vos WM, Fitzgerald GF, Ventura M, O'Toole PW, van Sinderen D. 2011. Functional genome analysis of *Bifidobacterium breve* UCC2003 reveals type IVb tight adherence (Tad) pili as an

749 essential and conserved host-colonization factor. Proc Natl Acad Sci U S A
750 108:11217–11222.
751 66. Zhu A, Sunagawa S, Mende DR, Bork P. 2015. Inter-individual differences in the
752 gene content of human gut bacterial species. Genome Biol 16:82.
753 67. Yawata Y, Kiyokawa T, Kawamura Y, Hirayama T, Takabe K, Nomura N. 2019. Intra-
754 and interspecies variability of single-cell innate fluorescence signature of microbial
755 cell. Appl Environ Microbiol 85.
756 68. Seed KD, Faruque SM, Mekalanos JJ, Calderwood SB, Qadri F, Camilli A. 2012.
757 Phase variable O antigen biosynthetic genes control expression of the major
758 protective antigen and bacteriophage receptor in *Vibrio cholerae* O1. PLoS Pathog
759 8:e1002917.
760 69. Chen C-C, Liou J-M, Lee Y-C, Hong T-C, El-Omar EM, Wu M-S. 2021. The
761 interplay between *Helicobacter pylori* and gastrointestinal microbiota. Gut Microbes
762 13:1–22.
763 70. Malfertheiner P, Camargo MC, El-Omar E, Liou J-M, Peek R, Schulz C, Smith SI,
764 Suerbaum S. 2023. *Helicobacter pylori* infection. Nat Rev Dis Primers 9:19.
765 71. Chaturvedi R, de Sablet T, Asim M, Piazuelo MB, Barry DP, Verriere TG, Sierra JC,
766 Hardbower DM, Delgado AG, Schneider BG, Israel DA, Romero-Gallo J, Nagy TA,
767 Morgan DR, Murray-Stewart T, Bravo LE, Peek RM Jr, Fox JG, Woster PM, Casero
768 RA Jr, Correa P, Wilson KT. 2015. Increased *Helicobacter pylori*-associated gastric
769 cancer risk in the Andean region of Colombia is mediated by spermine oxidase.
770 Oncogene 34:3429–3440.
771 72. Shirani M, Pakzad R, Haddadi MH, Akrami S, Asadi A, Kazemian H, Moradi M,
772 Kaviar VH, Zomorodi AR, Khoshnood S, Shafieian M, Tavasolian R, Heidary M,
773 Saki M. 2023. The global prevalence of gastric cancer in *Helicobacter pylori*-
774 infected individuals: a systematic review and meta-analysis. BMC Infect Dis 23:543.
775 73. Tacconelli E, Carrara E, Savoldi A, Harbarth S, Mendelson M, Monnet DL, Pulcini
776 C, Kahlmeter G, Kluytmans J, Carmeli Y, Ouellette M, Outterson K, Patel J, Cavaleri
777 M, Cox EM, Houchens CR, Grayson ML, Hansen P, Singh N, Theuretzbacher U,
778 Magrini N, Aboderin AO, Al-Abri SS, Awang Jalil N, Benzonana N, Bhattacharya S,
779 Brink AJ, Burkert FR, Cars O, Cornaglia G, Dyar OJ, Friedrich AW, Gales AC,
780 Gandra S, Giske CG, Goff DA, Goossens H, Gottlieb T, Guzman Blanco M,
781 Hryniewicz W, Kattula D, Jinks T, Kanj SS, Kerr L, Kieny M-P, Kim YS, Kozlov RS,
782 Labarca J, Laxminarayan R, Leder K, Leibovici L, Levy-Hara G, Littman J,
783 Malhotra-Kumar S, Manchanda V, Moja L, Ndoye B, Pan A, Paterson DL, Paul M,
784 Qiu H, Ramon-Pardo P, Rodríguez-Baño J, Sanguinetti M, Sengupta S, Sharland M,

785 Si-Mehand M, Silver LL, Song W, Steinbakk M, Thomsen J, Thwaites GE, van der
786 Meer JWM, Van Kinh N, Vega S, Villegas MV, Wechsler-Fördös A, Wertheim HFL,
787 Wesangula E, Woodford N, Yilmaz FO, Zorzet A. 2018. Discovery, research, and
788 development of new antibiotics: the WHO priority list of antibiotic-resistant bacteria
789 and tuberculosis. Lancet Infect Dis 18:318–327.
790 74. de Brito BB, da Silva FAF, Soares AS, Pereira VA, Santos MLC, Sampaio MM,
791 Neves PHM, de Melo FF. 2019. Pathogenesis and clinical management of
792 *Helicobacter pylori* gastric infection. World J Gastroenterol 25:5578–5589.
793 75. Chan BK, Abedon ST. 2012. Phage therapy pharmacology phage cocktails. Adv Appl
794 Microbiol 78:1–23.
795 76. Kortright KE, Chan BK, Koff JL, Turner PE. 2019. Phage therapy: a renewed
796 approach to combat antibiotic-resistant bacteria. Cell Host Microbe 25:219–232.
797 77. Lin DM, Koskella B, Lin HC. 2017. Phage therapy: an alternative to antibiotics in
798 the age of multi-drug resistance. World J Gastrointest Pharmacol Ther 8:162–173.
799 78. Loc-Carrillo C, Abedon ST. 2011. Pros and cons of phage therapy. Bacteriophage
800 1:111–114.
801 79. Pires Diana P., Cleto Sara, Sillankorva Sanna, Azeredo Joana, Lu Timothy K. 2016.
802 Genetically engineered phages: a review of advances over the last decade. Microbiol
803 Mol Biol Rev 80:523−543.
804 80. Abedon ST, Kuhl SJ, Blasdel BG, Kutter EM. 2011. Phage treatment of human
805 infections. Bacteriophage 1:66–85.
806 81. Balogh B, Jones JB, Iriarte FB, Momol MT. 2010. Phage therapy for plant disease
807 control. Curr Pharm Biotechnol 11:48–57.
808 82. Loc Carrillo C, Atterbury RJ, el-Shibiny A, Connerton PL, Dillon E, Scott A,
809 Connerton IF. 2005. Bacteriophage therapy to reduce *Campylobacter jejuni*
810 colonization of broiler chickens. Appl Environ Microbiol 71:6554–6563.
811 83. Tanji Y, Shimada T, Yoichi M, Miyanaga K, Hori K, Unno H. 2004. Toward rational
812 control of *Escherichia coli* O157:H7 by a phage cocktail. Appl Microbiol Biotechnol
813 64:270–274.
814 84. Gu J, Liu X, Li Y, Han W, Lei L, Yang Y, Zhao H, Gao Y, Song J, Lu R, Sun C, Feng
815 X. 2012. A method for generation phage cocktail with great therapeutic potential.
816 PLoS One 7:e31698.
817 85. Holder KK, Bull JJ. 2001. Profiles of adaptation in two similar viruses. Genetics
818 159:1393–1404.
819 86. Cox J, Schubert AM, Travisano M, Putonti C. 2010. Adaptive evolution and inherent

820 tolerance to extreme thermal environments. BMC Evol Biol 10:75.
821 87. Kering KK, Zhang X, Nyaruaba R, Yu J, Wei H. 2020. Application of adaptive
822 evolution to improve the stability of bacteriophages during storage. Viruses 12:423.
823 88. Borges AL. 2021. How to train your bacteriophage. Proc Natl Acad Sci U S A.
824 89. Borin JM, Avrani S, Barrick JE, Petrie KL, Meyer JR. 2021. Coevolutionary phage
825 training leads to greater bacterial suppression and delays the evolution of phage
826 resistance. Proc Natl Acad Sci U S A 118.
827 90. Cheng H, Concepcion GT, Feng X, Zhang H, Li H. 2021. Haplotype-resolved de
828 novo assembly using phased assembly graphs with hifiasm. Nat Methods 18:170–
829 175.
830 91. Li H. 2018. Minimap2: pairwise alignment for nucleotide sequences. Bioinformatics
831 34:3094–3100.
832 92. Nurk S, Walenz BP, Rhie A, Vollger MR, Logsdon GA, Grothe R, Miga KH, Eichler
833 EE, Phillippy AM, Koren S. 2020. HiCanu: accurate assembly of segmental
834 duplications, satellites, and allelic variants from high-fidelity long reads. Genome
835 Res 30:1291–1305.
836 93. Hyatt D, Chen G-L, Locascio PF, Land ML, Larimer FW, Hauser LJ. 2010. Prodigal:
837 prokaryotic gene recognition and translation initiation site identification. BMC
838 Bioinformatics 11:119.
839 94. Buchfink B, Xie C, Huson DH. 2015. Fast and sensitive protein alignment using
840 DIAMOND. Nat Methods 12:59–60.
841 95. Roberts RJ, Vincze T, Posfai J, Macelis D. 2015. REBASE--a database for DNA
842 restriction and modification: enzymes, genes and genomes. Nucleic Acids Res
843 43:D298-9.
844 96. Payne LJ, Todeschini TC, Wu Y, Perry BJ, Ronson CW, Fineran PC, Nobrega FL,
845 Jackson SA. 2021. Identification and classification of antiviral defence systems in
846 bacteria and archaea with PADLOC reveals new system types. Nucleic Acids Res
847 49:10868–10878.
848 97. Jain C, Rodriguez-R LM, Phillippy AM, Konstantinidis KT, Aluru S. 2018. High
849 throughput ANI analysis of 90K prokaryotic genomes reveals clear species
850 boundaries. Nat Commun 9:5114.
851 98. Cui Z, Cui Y, Zang T, Wang Y. 2021. interacCircos: an R package based on JavaScript
852 libraries for the generation of interactive circos plots. Bioinformatics 37:3642–3644.

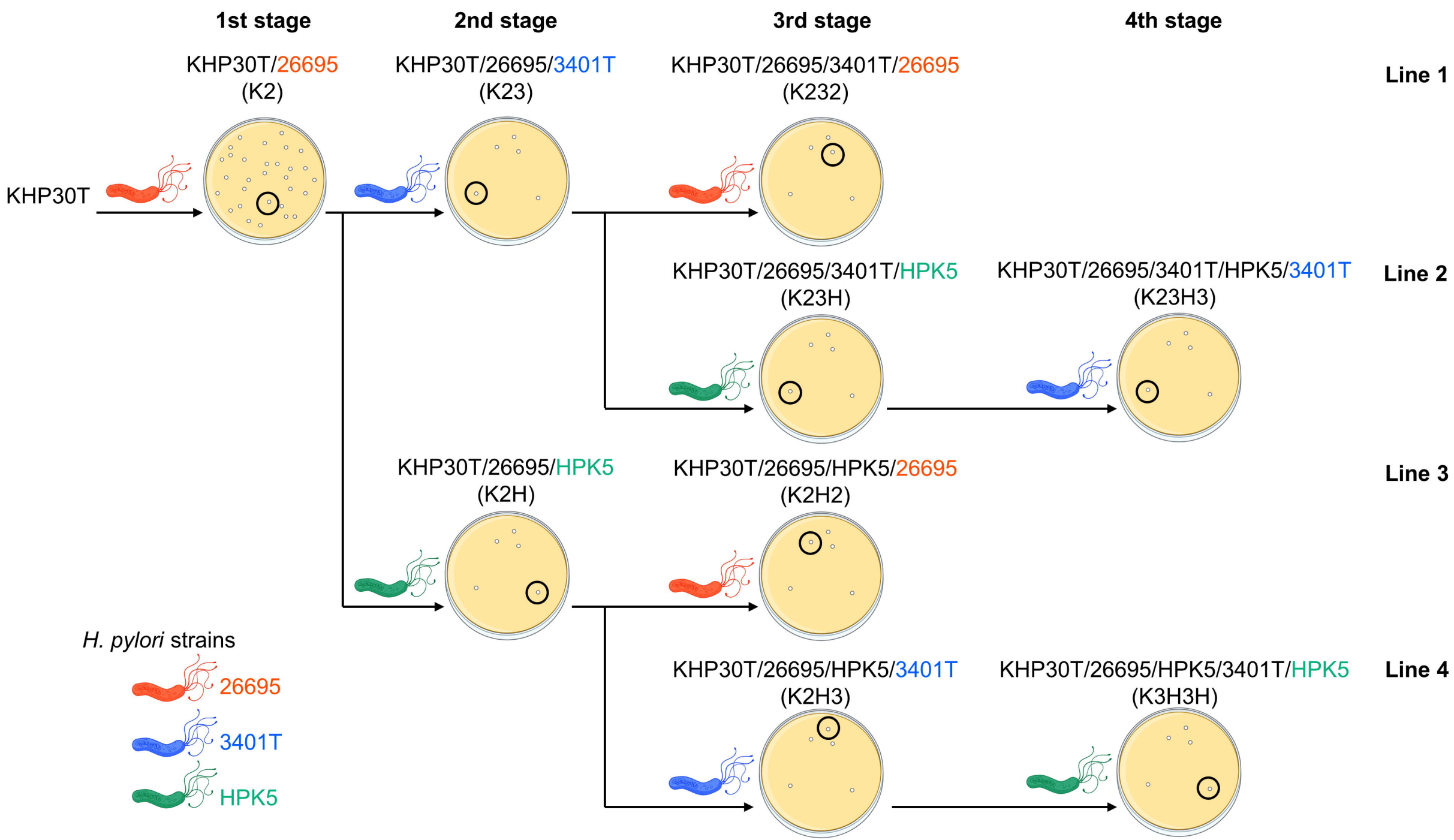
1st stage
2nd stage
3rd stage
4th stage
KHP30T
KHP30T/26695
(K2)
KHP30T/26695/3401T
(K23)
KHP30T/26695/3401T/26695
(K232)
Line 1
KHP30T/26695/3401T/HPK5
(K23H)
KHP30T/26695/3401T/HPK5/3401T
(K23H3)
Line 2
KHP30T/26695/HPK5
(K2H)
KHP30T/26695/HPK5/26695
(K2H2)
Line 3
KHP30T/26695/HPK5/3401T
(K2H3)
KHP30T/26695/HPK5/3401T/HPK5
(K3H3H)
Line 4
H. pylori strains
26695
3401T
HPK5

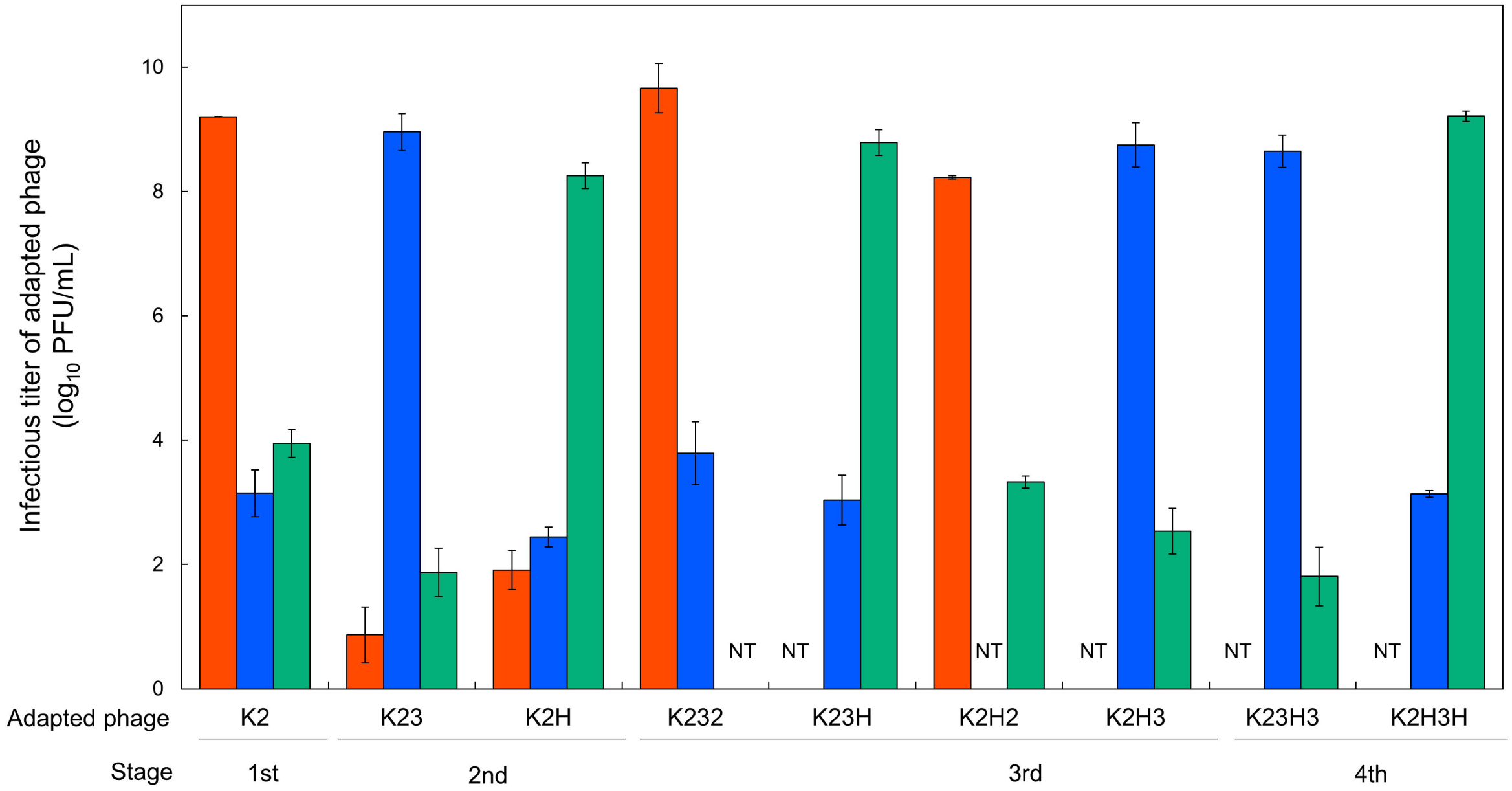
Infectious titer of adapted phage
(log10 PFU/mL)
10
8
6
4
2
0
NT
NT
NT
NT
NT
NT
Adapted phage
K2
K23
K2H
K232
K23H
K2H2
K2H3
K23H3
K2H3H
Stage
1st
2nd
3rd
4th

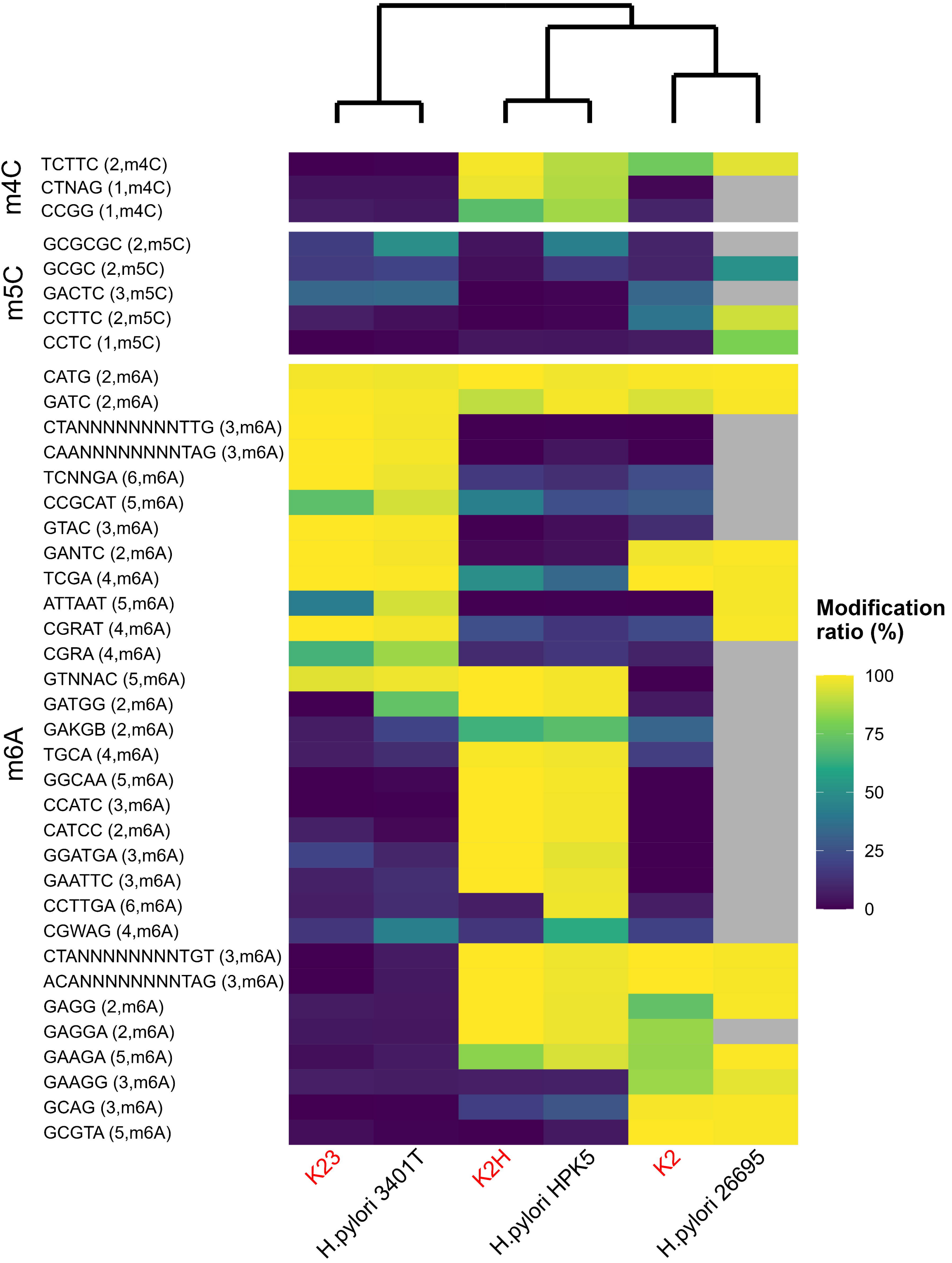
m4C
TCTTC (2,m4C)
CTNAG (1,m4C)
CCGG (1,m4C)
m5C
GCGCGC (2,m5C)
GCGC (2,m5C)
GACTC (3,m5C)
CCTTC (2,m5C)
CCTC (1,m5C)
m6A
CATG (2,m6A)
GATC (2,m6A)
CTANNNNNNNNTTG (3,m6A)
CAANNNNNNNNTAG (3,m6A)
TCNNGA (6,m6A)
CCGCAT (5,m6A)
GTAC (3,m6A)
GANTC (2,m6A)
TCGA (4,m6A)
ATTAAT (5,m6A)
CGRAT (4,m6A)
CGRA (4,m6A)
GTNNAC (5,m6A)
GATGG (2,m6A)
GAKGB (2,m6A)
TGCA (4,m6A)
GGCAA (5,m6A)
CCATC (3,m6A)
CATCC (2,m6A)
GGATGA (3,m6A)
GAATTC (3,m6A)
CCTTGA (6,m6A)
CGWAG (4,m6A)
CTANNNNNNNNTGT (3,m6A)
ACANNNNNNNNTAG (3,m6A)
GAGG (2,m6A)
GAGGA (2,m6A)
GAAGA (5,m6A)
GAAGG (3,m6A)
GCAG (3,m6A)
GCGTA (5,m6A)
Modification ratio (%)
100
75
50
25
0
K23
H.pylori 3401T
K2H
H.pylori HPK5
K2
H.pylori 26695